

# *Cynodon dactylon* Leaf Extract Assisted Green Synthesis of Silver Nanoparticles and Their Anti-Microbial Activity

R. K. Sharma<sup>1,\*</sup>, S. Tahiliani<sup>1</sup>, N. Jain<sup>1</sup>, R. Priyadarshi<sup>1</sup>,  
S. Chhangani<sup>1</sup>, S. D. Purohit<sup>1</sup>, and Prachi Joshi<sup>2,\*</sup>

<sup>1</sup>Centre for Converging Technologies, University of Rajasthan, Jaipur, Rajasthan, India

<sup>2</sup>Bharti Vidyapeeth's College of Engineering, Paschim Vihar, New Delhi, India

A facile green synthesis of silver nanoparticles (AgNPs) using the leaf extract of *Cynodon dactylon* (Bermuda grass) is reported. The reduction of silver ions into AgNPs by *Cynodon dactylon* grass leaf extract was observed by the color change of solution from yellowish brown to dark brown. The formation of AgNPs was confirmed by the characteristic surface plasmon resonance absorption band in the visible region using UV-Visible absorption spectroscopy. The size and morphology of nanoparticles were determined by the transmission electron microscopy (TEM) measurement and the average size of spherical nanoparticles was observed to be ~20 nm. The lattice fringe spacing in AgNPs was found to be ~0.20 nm attributed to the (200) crystal plane of face-centered cubic silver and the reflections in electron diffraction pattern suggested the polycrystalline nature of nanoparticles. The FTIR measurement evidenced the presence of biomolecules at the surface of AgNPs suggesting that the biomolecules presents in the leaf extract act as reducing agent as well as the capping agent for AgNPs. The as synthesized AgNPs were found to exhibit strong anti-microbial activity against both *Escherichia coli* (*E.coli*) bacteria and *Candida albicans* (*C. albicans*) fungus implying their strong potential as antimicrobial agent.

**KEYWORDS:** Silver Nanoparticles, Green Synthesis, *Cynodon dactylon*, Anti-Microbial Activity, *Escherichia coli*, *Candida albicans*.

## 1. INTRODUCTION

Nanostructured silver particles, owing to their extraordinary properties, have been widely exploited for several technological applications from photonics, electronics, and catalysis to various biomedical applications.<sup>1–4</sup> The interest for silver nanoparticles (AgNPs) lies in their distinct properties such as conductivity, stability, catalytic, anti-bacterial and anti-fungal properties.<sup>5–8</sup> Additionally, the unique surface plasmon resonance absorption of AgNPs imparts an extraordinary feature to the particles to be utilized in surface enhanced raman spectroscopy providing great opportunity for medical diagnostics and imaging.<sup>9</sup>

Silver has been known to exhibit toxicity towards variety of micro-organisms and several silver salts are commercially used as anti-microbial agents.<sup>10</sup> Silver based ointments and bandages for wound healing have already

been proven to be effective against bacterial infections.<sup>11</sup> However, the AgNPs are found to be more effective than their Ag<sup>+</sup> counterparts<sup>12</sup> and have found applications in antimicrobial paint coatings,<sup>13</sup> textiles, water treatment, and medical devices.<sup>14</sup> The anti-microbial activity of nanoparticles has been correlated to their ability to interact or penetrate the cell wall of bacteria and generation of reactive oxygen species (ROS).<sup>5, 15–17</sup> The antimicrobial activity of AgNPs has been studied by various research groups on variety of micro-organisms.<sup>18–22</sup> AgNPs have been found to be effective against gram positive, gram negative and some of the multiresistant strains such as *Staphylococcus aureus*, *Escherichia coli*, *Salmonella enteric*, methicillin-resistant *Staphylococcus aureus*.<sup>18–22</sup>

Chemical reduction of silver ions using borohydride, citrate and ascorbate as reductants is the most frequently used method for the formation of AgNPs.<sup>23–25</sup> However, chemical reduction is preferably performed in presence of stabilizers such as polymers, dendrimers and alkanethiols in order to prevent aggregation and control the size and shape of nanoparticles.<sup>26–28</sup> With growing concerns over

\* Authors to whom correspondence should be addressed.  
Emails: krishnasharma01@gmail.com, dr.prjoshi@yahoo.com  
Received: xx XXXX XXXX  
Accepted: xx XXXX XXXX

biological and environmental impact of nanomaterials, the need of applying green synthesis techniques for nanoparticles has increased significantly.<sup>29,30</sup> The green synthesis of AgNPs involves polysaccharide method, Tollens method, irradiation method, polyoxometalates and biological methods.<sup>25</sup> The biologically stimulated syntheses of AgNPs using different micro-organisms, fungus and plant extracts have been significantly recognized as green nanotechnology approach for making biocompatible and environment friendly nanoparticles.<sup>31–34</sup> For example, the AgNPs have been reported to be produced by utilizing *Pseudomonas stutzeri* AG259 bacterium,<sup>31</sup> *Fusarium oxysporum* and *Phanerochaete chrysosporium* fungus<sup>32,33</sup> etc.

However, synthesis of AgNPs using plants/plant extracts is considered to be more advantageous over other biological methods as it avoids maintenance of cell cultures, and found to be suitable for large scale synthesis of nanoparticles.<sup>34</sup> The plant extracts from live alfalfa, lemon-grass, amla, aloe vera, curry leaves, neem, tea polyphenols, and others have been successfully used as green reductants in AgNPs synthesis; wherein the reduction and stabilization of metal ions have been attributed to the polyol components and water soluble heterocyclic components of extracts.<sup>35–41</sup> In the present work, we present a rapid green synthesis of AgNPs using *Cynodon dactylon* (Bermuda grass) leaf extract and studied its anti-microbial activity on gram negative *Escherichia coli* (*E.coli*) bacteria and *Candida albicans* (*C.albicans*) fungus. The anti-microbial experiments were carried out using Kirby-Bauer disc diffusion method.

## 2. MATERIALS AND METHODS

### 2.1. Plant Material and Preparation of the Extract

The leaves of *Cynodon dactylon* (Bermuda grass) were collected to prepare the aqueous plant extract. The leaves were meticulously washed in distilled followed by crushing 10 g of grass leaves in 100 ml of distilled water. The crushed leaves were then centrifuged at 10,000 rpm for 20 minutes. The supernatant was collected subsequently and filtered using whatman no. 1 filter paper.

### 2.2. Synthesis of AgNPs

Silver nitrate ( $\geq 99.0\%$ ) was purchased from Sigma-Aldrich and used without further purifications. 1 mM solution of silver nitrate was prepared in double distilled water. The freshly prepared supernatant of grass leaf extract was added to the aqueous silver nitrate solution in 1:9 ratio. The temperature of the mixture was raised to 60 °C and kept constant for 15–20 minutes. The change in color of the solution indicated the reduction of Ag<sup>+</sup> ions. The prepared AgNPs were then subjected to various characterizations.

### 2.3. UV-Vis Spectroscopy

The formation of AgNPs was verified by determining optical density from UV-Vis absorption spectroscopy. The characteristic surface plasmon absorption band of colloidal silver nanoparticles is observed in the visible range. The optical density spectra were recorded using UV-1800 spectrophotometer (Shimadzu, Japan) and the optical response was taken from 300–800 nm range in a 10 mm path quartz cuvette. A small aliquot of the AgNPs solution was diluted into distilled water before taking to UV-Vis measurement.

### 2.4. Dynamic Light Scattering (DLS)

The hydrodynamic radius of nanoparticles in aqueous solution was determined using Viscotek 802 dynamic light scattering instrument. The scattered light coming from a 50 mW laser source of 830 nm was recorded from an internal light detector aligned at 90° from the source. The sample (60  $\mu$ l AgNPs in DI water) in 50 mM sodium phosphate buffer of pH 7.6 was placed in a quartz cuvette and measurement was carried out at a constant temperature of 25 °C.

### 2.5. FTIR Analysis

FTIR scanning was preferred in the transmission mode with constant nitrogen purging. FTIR spectrum of dried sample was recorded using Fourier Transform Infra Red Spectrophotometer (FTIR-8101A) Shimadzu, Japan in KBr medium in the range of 4600–400 cm<sup>-1</sup> at room temperature. The sample of AgNPs was vacuum dried and 1–2 mg of fine sample powder was mixed with 90–100 mg of KBr powder. The KBr used as scanning matrix was of IR grade. The mixer was dehumidified completely using dry box and then transferred to a 13 mm die to make a nearly transparent and homogeneous pallet.

### 2.6. Transmission Electron Microscopy (TEM)

The particle size and dispersity of the prepared nanoparticles were studied using transmission electron microscope (TEM). Freshly prepared AgNPs solution was 10 times diluted using distilled water and 5  $\mu$ L of it was placed on copper grid. The sample containing TEM grid was dried at room temperature completely. The bright field electron micrographs were obtained with a JEOL JEM-2100F transmission electron microscope equipped with Gatan Orius SC 1000 (2 k × 4 k) at the accelerating voltage of 200 kV. The sample containing TEM grid was kept in dust free atmosphere.

### 2.7. Antimicrobial Activity of Silver Nanoparticles

The anti-microbial activity of AgNPs was studied using Kirby-Bauer disc diffusion method. The anti-bacterial

activity of AgNPs was studied against gram negative *E.coli* bacteria. The plates containing Luria Bertani (LB) agar medium were sterilized and solidified. Approximately  $10^6$  colony forming units (CFU) were spread on LB agar plates to cultivate the bacteria. The sterilized filter paper discs of 5 mm diameter were dipped in AgNPs solutions of varying concentrations ( $1-5 \mu\text{g/ml}$ ) and placed in agar plates. One disc was dipped in  $1 \text{ mM AgNO}_3$  solution and considered as control. The plates were then incubated at  $37^\circ\text{C}$  for 24 hours. The zones of inhibition for control and AgNPs were measured.

For the anti-fungal activity of AgNPs, the Potato dextrose agar (PDA) medium was used to grow the fungi *C.albicans*. The fungal culture was swabbed on sterilized and solidified agar plates. The sterilized paper discs dipped in AgNPs solutions ( $1-4 \mu\text{g/ml}$ ) were impregnated in each Petri plate of culture and zones of inhibition were measured. One disc was dipped in  $1 \text{ mM AgNO}_3$  solution for control. The experiments were repeated thrice and the average was taken.

### 3. RESULTS AND DISCUSSION

#### 3.1. Formation of AgNPs and Their Characterization

The AgNPs have been prepared by the reduction of silver nitrate in aqueous medium by using *Cynodon dactylon* grass leaf extract. The reduction of silver nitrate is attributed to the metabolites i.e., proteins, flavonoids and alkanoids present in the *Cynodon dactylon* plant extract.<sup>42</sup> As the grass leaf extract was added to the silver nitrate mixture and heated, the color of the mixture changes rapidly from light yellowish-brown to dark brown and then the color did not change any more with reaction time [Fig. 1].<sup>43</sup> The formation of AgNPs is confirmed by the optical absorption measurement using UV-Vis spectroscopy. The characteristic surface plasmon resonance (SPR) absorption



**Fig. 1.** Formation of AgNPs using *Cynodon dactylon* leaf extract: (a) *Cynodon dactylon* grass leaf extract (yellow); (b) Silver nitrate solution with *Cynodon dactylon* grass leaf extract at 0 mins (yellowish-brown); and (c) Formation of AgNPs after 20 mins of mixing (dark brown).

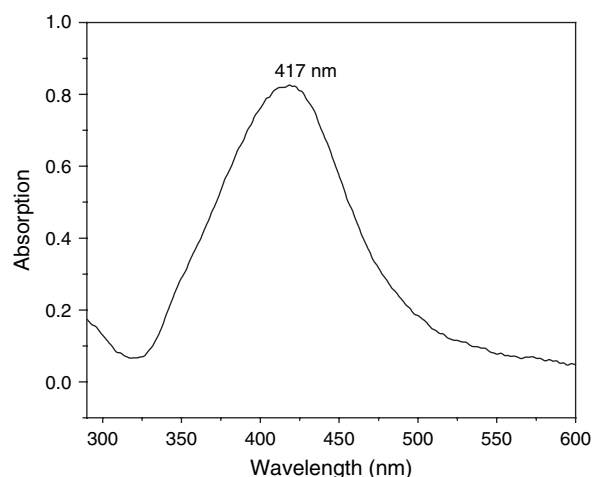


**Fig. 2.** Representative UV-vis absorption spectrum of AgNPs after 20 minutes of addition of *Cynodon dactylon* grass leaf extract to the silver nitrate solution.

band for AgNPs has been observed at 419 nm of electromagnetic spectrum suggesting the successful formation of AgNPs [Fig. 2].<sup>44,45</sup> Figure 2 shows the optical absorption of AgNPs after 20 minutes of mixing of silver nitrate with grass leaf extract at elevated temperature.

The size and dispersity of synthesized AgNPs were determined by using high resolution transmission electron microscope (HRTEM) and the results are presented in Figure 3. The HRTEM image in Figure 3(a) suggests that the AgNPs are spherical in shape with an average size  $\sim 20 \text{ nm}$ . The size distribution is found to be nearly uniform, however, the particles are seems to be interconnected through some kind of surface network. It is also noticeable that the edges of the particles appear comparatively are lighter suggesting the presence of biomolecules (proteins, alkanoids) at the surface of AgNPs. As the nanoparticles were synthesized using grass leaf extract containing metabolites (proteins, flavonoids, alkanoids), these species may therefore result in the formation of such kind of network. The high resolution micrograph in Figure 3(b) shows the lattice fringe pattern of AgNPs indicating the lattice spacing  $\sim 0.20 \text{ nm}$  corresponding to the (200) plane of face-centered cubic (fcc) silver. The electron diffraction pattern of AgNPs in Figure 3(c) shows the polycrystalline nature of nanoparticles and the diffraction rings from inner to outer could be indexed as (111), (200), (220), (311), and (222) reflections respectively corresponding to fcc silver (JCPDS 04-0783).<sup>46</sup>

The radius of hydration of AgNPs in aqueous medium was measured by using DLS and found to be  $78.66 \pm 8.09 \text{ nm}$  as shown in Figure 4. It is noticed that the size of AgNPs using DLS is found to be higher in comparison to the size measured by HRTEM. DLS measures the hydrodynamic radii of particles in solution, hence the size measured using DLS are more significant than HRTEM for samples to be used for biomedical applications.

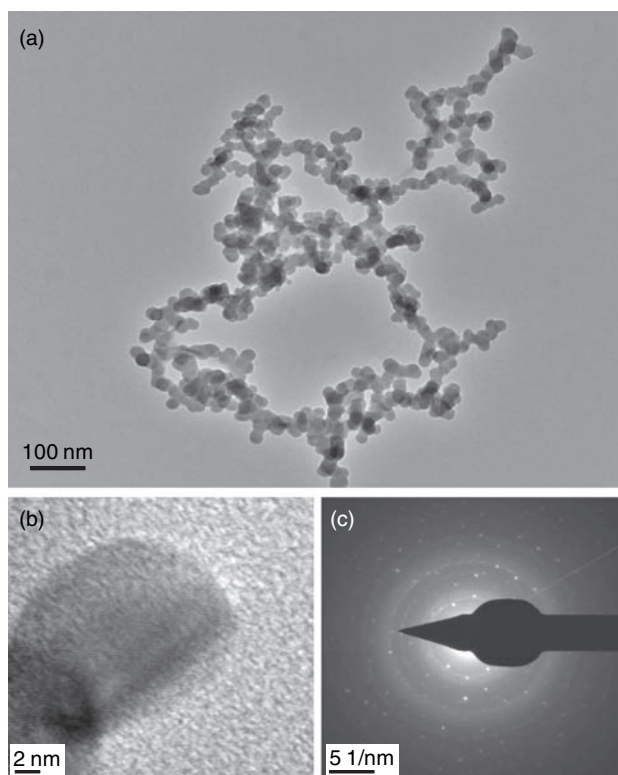


**Fig. 3.** (a) HRTEM micrograph of synthesized AgNPs; (b) Magnified HRTEM micrograph of AgNPs showing the lattice fringe pattern; and (c) Electron diffraction pattern of AgNPs.

In order to determine the moieties present at the surface of AgNPs, FTIR measurement was done in KBr medium and the result is shown in Figure 5. The peak obtained at  $3425\text{ cm}^{-1}$  is attributed to the O—H stretching in phenols and alcohols. The peak at  $2958\text{ cm}^{-1}$  and  $2902\text{ cm}^{-1}$  are assigned to O—H stretching of carboxylic acids and C—H stretching in alkanes respectively. The band at  $1705\text{ cm}^{-1}$  is due to the  $>\text{C}=\text{O}$  stretch of the phenolic esters and

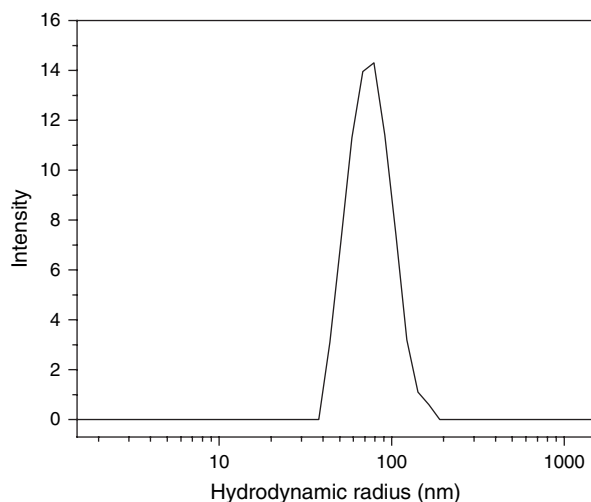


**Fig. 4.** Dynamic light scattering (DLS) measurement of AgNPs.

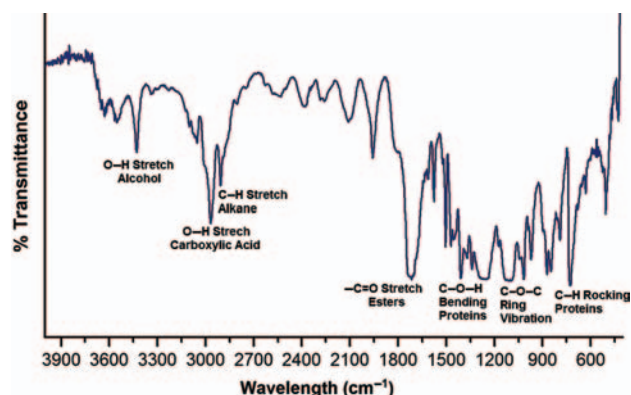


**Fig. 5.** FTIR spectrum of synthesized AgNPs in transmission mode.

the sharp peak at  $1401\text{ cm}^{-1}$  corresponds to —C—O—H bending in carbohydrates and proteins of poaceae family. The bands in the range  $1200\text{--}600\text{ cm}^{-1}$  corresponds to the C—O—C ring vibrations in polysaccharides together with the C—H rocking of  $>\text{CH}_2$  in fatty acid chains and proteins.<sup>47</sup> The result suggests that the silver ions are reduced by the metabolites presents in the *Cynodon dactylon* plant such as proteins, carbohydrates, flavanoids, alkaloids, tri-terpenoides, glycosides etc. which subsequently get attach at the nanoparticles surface.<sup>42</sup>

### 3.2. Anti-Microbial Activity of AgNPs

The AgNPs synthesized by green route are found to show strong antimicrobial activities against the bacteria as well as the fungus [Fig. 6]. Figure 6(a) represents the anti-bacterial activity of AgNPs against *E.coli* and Figure 6(b) represents the anti-fungal activity of AgNPs against *C.albicans*. The results are summarized in Table I in the form of inhibition zone diameter created by the varying concentrations of AgNPs in comparison with the bare  $\text{AgNO}_3$  solution. In Figure 6(a), the disc 1 corresponds to the  $\text{AgNO}_3$  control and the discs 2, 3 and 4 correspond to 1.0, 2.0, and 5.0  $\mu\text{g/ml}$  of AgNPs. The inhibition zone

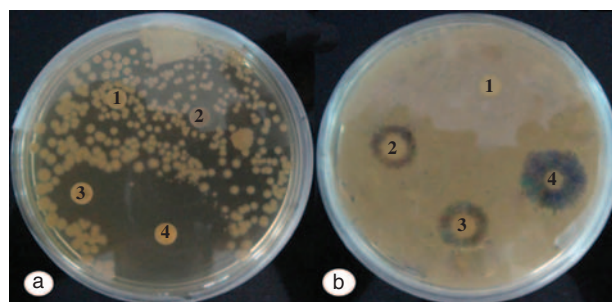


**Fig. 6.** Anti-microbial activity of AgNPs in terms of zone of inhibition created by AgNPs. (a) Anti-bacterial activity of AgNPs against *E.coli* bacteria where discs 1–4 correspond to control, 1.0  $\mu\text{g/ml}$ , 2.0  $\mu\text{g/ml}$  and 5.0  $\mu\text{g/ml}$  of AgNPs respectively; (b) Anti-fungal activity of AgNPs against *C.albicans* fungus, where discs 1–4 correspond to the control, 1.0  $\mu\text{g/ml}$ , 2.0  $\mu\text{g/ml}$  and 4.0  $\mu\text{g/ml}$  of AgNPs respectively.

**Table I.** Size of the inhibition zones for AgNPs synthesized by *Cynodon dactylon* against the tested microorganisms.

| <i>Escherichia coli</i> |                      |                      | <i>Candida albicans</i> |                      |                      |
|-------------------------|----------------------|----------------------|-------------------------|----------------------|----------------------|
| Discs                   | Sample               | Inhibition zone (mm) | Discs                   | Sample               | Inhibition zone (mm) |
| 1                       | Control              | 5                    | 1                       | Control              | 5                    |
| 2                       | 1.0 $\mu\text{g/ml}$ | 6                    | 2                       | 1.0 $\mu\text{g/ml}$ | 9                    |
| 3                       | 2.0 $\mu\text{g/ml}$ | 12                   | 3                       | 2.0 $\mu\text{g/ml}$ | 10                   |
| 4                       | 5.0 $\mu\text{g/ml}$ | 24                   | 4                       | 4.0 $\mu\text{g/ml}$ | 13                   |

diameters are found to be 6, 12, and 24 mm for 1.0, 2.0, and 5.0  $\mu\text{g/ml}$  of AgNPs test samples compared to 5 mm of  $\text{AgNO}_3$  control. It is clearly seen that the antibacterial activity of the AgNPs is increasing with increasing concentration. In Figure 6(b), the disc 1 corresponds to the  $\text{AgNO}_3$  control and the disc 2, 3, and 4 correspond to 1.0, 2.0, and 4.0  $\mu\text{g/ml}$  of AgNPs solution. The inhibition zone diameters are found to be 9, 10, and 13 mm for 1.0, 2.0, and 4.0  $\mu\text{g/ml}$  of AgNPs test samples compared to that of 5 mm of  $\text{AgNO}_3$  control. The increased inhibition zone diameters compared to that of control reveals the strong anti-microbial activity of AgNPs against the bacteria as well as the fungus.

The mechanism of anti-microbial activity of AgNPs is not fully understood yet, however it has been attributed to the increased cell membrane permeability and perturbed cell respiration functions on interaction of microorganisms with AgNPs.<sup>20</sup> The AgNPs with high surface energy may interact with cell wall constituents and damage the cell wall resulting into the penetration of nanoparticles inside the microorganism's cell. As the silver has high affinity towards the phosphorous and sulfur containing compounds, the AgNPs may therefore react with those biomolecules and perturb the cell functioning thereby causing cell death.<sup>48,49</sup> The release of silver ions from AgNPs has also been reported a cause of bacterial cell death.<sup>50</sup> Recently, it has been reported that oxygen is capable of oxidizing AgNPs to form partially oxidized AgNPs with surface adsorbed  $\text{Ag}^+$  ions, hence may contribute in enhanced anti-microbial activity of AgNPs.<sup>51</sup>

#### 4. CONCLUSION

The present study involved the green synthesis of AgNPs using *Cynodon dactylon* leaf extract and their anti-microbial activity. The spectroscopic and electron microscopy measurements revealed the successful formation of AgNPs. The FTIR measurement confirmed the presence of biomolecules at the surface of AgNPs, which came from the synthesis process of involving reduction of silver by *Cynodon dactylon* leaf extract. The anti-microbial activity measurements suggest that the AgNPs have strong toxic potential towards bacteria (*E.coli*) as well as the fungus (*C.albicans*). The high bioavailability of the grass

makes this method easy, economically viable and useful for large scale production. As the anti-microbial properties of silver have been utilized into variety of medical applications such as AgNPs coated plastic catheters, polymethyl-metacrylate bone cement and paints etc. The green route of AgNPs formation would significantly enhance their therapeutic efficacy and biomedical potential.

#### References and Notes

- P. M. Hosel and F. C. Krebs, *J. Mater. Chem.* 22, 15683 (2012).
- Y. Li, Y. Wu, and B. S. Ong, *J. Am. Chem. Soc.* 127, 3266 (2005).
- A. Murugadoss and A. Chattopadhyay, *Nanotechnol.* 19, 015603 (2008).
- M. Ahamed, M. S. Alsalhi, and M. K. J. Siddiqui, *Clin. Chim. Acta* 411, 1841 (2010).
- C. Carlson, S. M. Hussain, A. M. Schrand, L. K. Braydich-Stolle, K. L. Hess, R. L. Jones, and J. J. Schlager, *J. Phys. Chem. B* 112, 13608 (2008).
- P. Mukherjee, A. Ahmad, D. Mandal, S. Senapati, S. R. Sainkar, M. I. Khan, R. Kumar, and M. Sastry, *Nano Lett.* 1, 515 (2001).
- I. Sondi and S. S. Branka, *J. Colloid Interface Sci.* 275, 177 (2004).
- X. Chen and H. J. Schluesener, *Toxicol. Lett.* 176, 1 (2008).
- N. L. Rosi and C. A. Mirkin, *Chem. Rev.* 105, 1547 (2005).
- Q. L. Feng, J. Wu, G. Q. Chen, F. Z. Cui, T. N. Kim, and J. O. Kim, *J. Biomed. Mater. Res.* 52, 662 (2000).
- J. P. Chen, *J. Invasive Cardiol.* 19, 395 (2007).
- C. N. Lok, C. M. Ho, R. Chen, Q. Y. He, W. Y. Yu, H. Sun, P. K. H. Tam, J. F. Chiu, and C. M. Che, *J. Proteome Res.* 5, 916 (2006).
- A. Kumar, P. K. Vemula, P. M. Ajayan, and G. John, *Nature* 7, 236 (2008).
- R. A. Khaydarov, R. R. Khaydarov, O. Gapurova, Y. Estrin, and T. J. Scheper, *Nanopart. Res.* 11, 1193 (2008).
- L. Braydich-Stolle, S. Hussain, J. J. Schlager, and M. C. Hofmann, *Toxicol. Sci.* 88, 412 (2005).
- P. Joshi, S. Chakraborti, P. Chakrabarti, D. Haranath, V. Shanker, Z. A. Ansari, S. P. Singh, and V. Gupta, *J. Nanosci. Nanotechnol.* 9, 6427 (2009).
- P. Joshi, S. Chakraborti, P. Chakrabarti, S. P. Singh, Z. A. Ansari, M. Husain, and V. Shanker, *Sci. Adv. Mater.* 4, 173 (2012).
- A. Panacek, L. Kvitek, R. Prucek, M. Kolar, R. Vecerova, N. Pizurova, V. K. Sharma, T. Nevecna, and R. Zboril, *J. Phys. Chem. B* 110, 16248 (2006).
- P. Irwin, J. Martin, L. H. Nguyen, Y. He1, A. Gehring, and C. Y. Chen, *Journal of Nanobiotechnology* 8, 34 (2010).
- L. Kvitek, A. Panacek, J. Soukupova, M. Kolar, R. Vecerova, R. Prucek, M. Holecova, and R. Zboril, *J. Phys. Chem. C* 112, 5825 (2008).
- J. R. Morones, J. L. Elechiguerra, A. Camacho, K. Holt, J. Kouri, J. T. Ramirez, and M. J. Yacaman, *Nanotechnol.* 16, 2346 (2005).
- P. L. Carpenter, *Microbiology*, W. B. Saunders Company, Philadelphia (1972), p. 245.
- P. C. Lee and D. Meisel, *J. Phys. Chem.* 86, 3391 (1982).
- T. S. Ahmadi, Z. L. Wang, T. C. Green, A. Henglein, and M. El-Sayed, *Science* 272, 1924 (1996).
- V. K. Sharma, R. A. Yngard, and Y. Lin, *Adv. Colloid Interface Sci.* 145, 83 (2009).
- M. J. Hostetler, S. J. Green, J. J. Stokes, and R. W. Murray, *J. Am. Chem. Soc.* 118, 4212 (1996).
- D. V. Left, L. Brandt, and J. R. Heath, *Langmuir* 12, 4723 (1996).
- P. Joshi, Z. A. Ansari, S. P. Singh, and V. Shanker, *Adv. Sci. Lett.* 2, 360 (2009).
- P. T. Anastas and M. Poliakoff, *Nature* 413, 257 (2001).
- J. M. DeSimone, *Science* 297, 799 (2002).

31. T. Klaus, R. Joerger, E. Olsson, and C. G. Granqvist, *Proc. Natl. Acad. Sci. USA* 96, 13611 (1999).
32. A. Ahmad, S. Senapati, M. I. Khan, R. Kumar, R. Ramani, V. Srinivas, and M. Sastry, *Nanotechnology* 14, 824 (2003).
33. A. Vigneshwaran, A. A. Kathe, P. V. Varadarajan, R. P. Nachne, and R. H. Balasubramanya, *Colloids Surf. B. Biointerfaces* 53, 55 (2006).
34. S. S. Shanker, A. Rai, A. Ahmed, and M. Sastry, *J. Colloid Interface Sci.* 275, 496 (2004).
35. J. L. Gardea-Torresdey, E. Gomez, J. R. Peralta-Videa, J. G. Parsons, H. Troiani, and M. J. Yacaman, *Langmuir* 19, 1357 (2003).
36. S. S. Shankar, A. Ahmad, and M. Sastry, *Biotechnol. Prog.* 19, 1627 (2003).
37. B. Amkamwar, C. Damle, A. Ahmad, and M. Sastry, *J. Nanosci. Nanotechnol.* 5, 1665 (2005).
38. S. P. Chandran, M. Chaudhary, R. Pasricha, A. Ahmad, and M. Sastry, *Biotechnol. Prog.* 22, 577 (2000).
39. L. Christensen, S. Vivekanandhan, M. Misra, and A. K. Mohanty, *Adv. Mat. Lett.* 2, 429 (2011).
40. A. D. Dwivedi and K. Gopal, *Colloids and Surfaces A: Physico-chemical and Engineering Aspects* 369, 27 (2010).
41. M. C. Moulton, L. K. Braydich-Stolle, M. N. Nadagouda, S. Kunzelman, S. M. Hussain, and R. S. Varma, *Nanoscale* 2, 763 (2010).
42. V. M. Thakare, R. Y. Chaudhari, and V. R. Patil, *AJPSR* 1, 1 (2011).
43. B. J. Wiley, S. H. Im, Z. Y. Li, J. McLellan, A. Siekkinen, and Y. Xia, *J. Phys. Chem. B* 110, 15666 (2006).
44. V. C. Verma, R. N. Kharwar, and A. C. Gange, *Nanomedicine (Lond.)* 5, 33 (2010).
45. G. Li, D. He, Y. Qian, B. Guan, S. Gao, Y. Cui, K. Yokoyama, and L. Wang, *Int. J. Mol. Sci.* 13, 466 (2012).
46. D. Philip, C. Unni, S. A. Aromal, and V. K. Vidhu, *Spectrochim. Acta, Part A* 78, 899 (2011).
47. J. Parekh and S. V. Chanda, *Turk. J. Biol.* 31, 53 (2007).
48. D. W. Hatchert and S. J. Henry, *J. Phys. Chem.* 100, 9854 (1996).
49. S. Basu, S. Jana, S. Pande, and T. Pal, *J. Colloid Int. Sci.* 321, 288 (2008).
50. Y. Zhang, H. Peng, W. Huang, Y. Zhou, X. Zhang, and D. Yan, *J. Phys. Chem. C* 112, 2330 (2008).
51. C. N. Lok, C. M. Ho, R. Chen, Q. Y. He, W. Y. Yu, H. Sun, P. K. H. Tam, J. F. Chiu, and C. M. Che, *J. Biol. Inorg. Chem.* 12, 527 (2007).